First Searches for Axions and Axionlike Particles with the LUX Experiment

D. S. Akerib,[1,2,3] S. Alsum,[4] C. Aquino,[5] H. M. Araújo,[6] X. Bai,[7] A. J. Bailey,[6] J. Balajthy,[8] P. Beltrame,[5] E. P. Bernard,[9,10] A. Bernstein,[11] T. P. Biesiadzinski,[1,2,3] E. M. Boulton,[9,10] P. Brás,[12] D. Byram,[13,14] S. B. Cahn,[10] M. C. Carmona-Benitez,[15] C. Chan,[16] A. A. Chiller,[13] C. Chiller,[13] A. Currie,[6] J. E. Cutter,[17] T. J. R. Davison,[5] A. Dobi,[18] J. E. Y. Dobson,[19] E. Druszkiewicz,[20] B. N. Edwards,[10] C. H. Faham,[18] S. R. Fallon,[21] S. Fiorucci,[16,18] R. J. Gaitskell,[16] V. M. Gehman,[18] C. Ghag,[19] K. R. Gibson,[1] M. G. D. Gilchriese,[18] C. R. Hall,[8] M. Hanhardt,[7,14] S. J. Haselschwardt,[22] S. A. Hertel,[23] D. P. Hogan,[9] M. Horn,[14,9,10] D. Q. Huang,[16] C. M. Ignarra,[2,3] R. G. Jacobsen,[9] W. Ji,[1,2,3] K. Kamdin,[9] K. Kazkaz,[11] D. Khaitan,[20] R. Knoche,[8] N. A. Larsen,[10] C. Lee,[1,2,3] B. G. Lenardo,[17,11] K. T. Lesko,[18] A. Lindote,[12] M. I. Lopes,[12] A. Manalaysay,[17] R. L. Mannino,[24] M. F. Marzioni,[5,*] D. N. McKinsey,[9,18,10] D.-M. Mei,[13] J. Mock,[21] M. Moongweluwan,[20] J. A. Morad,[17] A. St. J. Murphy,[5] C. Nehrkorn,[22] H. N. Nelson,[22] F. Neves,[12] K. O'Sullivan,[9,18,10] K. C. Oliver-Mallory,[9] K. J. Palladino,[4,2,3] E. K. Pease,[9,10] L. Reichhart,[19] C. Rhyne,[16] S. Shaw,[19] T. A. Shutt,[1,2,3] C. Silva,[12] M. Solmaz,[22] V. N. Solovov,[12] P. Sorensen,[18] S. Stephenson,[17] T. J. Sumner,[6] M. Szydagis,[21] D. J. Taylor,[14] W. C. Taylor,[16] B. P. Tennyson,[10] P. A. Terman,[24] D. R. Tiedt,[7] W. H. To,[1,2,3] M. Tripathi,[17] L. Tvrznikova,[9,10] S. Uvarov,[17] V. Velan,[9] J. R. Verbus,[16] R. C. Webb,[24] J. T. White,[24] T. J. Whitis,[1,2,3] M. S. Witherell,[18] F. L. H. Wolfs,[20] J. Xu,[11] K. Yazdani,[6] S. K. Young,[21] and C. Zhang[13]

(LUX Collaboration)

[1]*Case Western Reserve University, Department of Physics, 10900 Euclid Avenue, Cleveland, Ohio 44106, USA*
[2]*SLAC National Accelerator Laboratory, 2575 Sand Hill Road, Menlo Park, California 94205, USA*
[3]*Kavli Institute for Particle Astrophysics and Cosmology, Stanford University, 452 Lomita Mall, Stanford, California 94309, USA*
[4]*University of Wisconsin-Madison, Department of Physics, 1150 University Avenue, Madison, Wisconsin 53706, USA*
[5]*SUPA, School of Physics and Astronomy, University of Edinburgh, Edinburgh EH9 3FD, United Kingdom*
[6]*Imperial College London, High Energy Physics, Blackett Laboratory, London SW7 2BZ, United Kingdom*
[7]*South Dakota School of Mines and Technology, 501 East St. Joseph Street, Rapid City, South Dakota 57701, USA*
[8]*University of Maryland, Department of Physics, College Park, Maryland 20742, USA*
[9]*University of California Berkeley, Department of Physics, Berkeley, California 94720, USA*
[10]*Yale University, Department of Physics, 217 Prospect Street, New Haven, Connecticut 06511, USA*
[11]*Lawrence Livermore National Laboratory, 7000 East Avenue, Livermore, California 94551, USA*
[12]*LIP-Coimbra, Department of Physics, University of Coimbra, Rua Larga, 3004-516 Coimbra, Portugal*
[13]*University of South Dakota, Department of Physics, 414E Clark Street, Vermillion, South Dakota 57069, USA*
[14]*South Dakota Science and Technology Authority, Sanford Underground Research Facility, Lead, South Dakota 57754, USA*
[15]*Pennsylvania State University, Department of Physics, 104 Davey Lab, University Park, Pennsylvania 16802-6300, USA*
[16]*Brown University, Department of Physics, 182 Hope Street, Providence, Rhode Island 02912, USA*
[17]*University of California Davis, Department of Physics, One Shields Avenue, Davis, California 95616, USA*
[18]*Lawrence Berkeley National Laboratory, 1 Cyclotron Road, Berkeley, California 94720, USA*
[19]*Department of Physics and Astronomy, University College London, Gower Street, London WC1E 6BT, United Kingdom*
[20]*University of Rochester, Department of Physics and Astronomy, Rochester, New York 14627, USA*
[21]*University at Albany, State University of New York, Department of Physics, 1400 Washington Avenue, Albany, New York 12222, USA*
[22]*University of California Santa Barbara, Department of Physics, Santa Barbara, California 93106, USA*
[23]*University of Massachusetts, Department of Physics, Amherst, Massachusetts 01003-9337 USA*
[24]*Texas A & M University, Department of Physics, College Station, Texas 77843, USA*

(Received 7 April 2017; published 29 June 2017)

The first searches for axions and axionlike particles with the Large Underground Xenon experiment are presented. Under the assumption of an axioelectric interaction in xenon, the coupling constant between axions and electrons g_{Ae} is tested using data collected in 2013 with an exposure totaling 95 live days $\times 118$ kg. A double-sided, profile likelihood ratio statistic test excludes g_{Ae} larger than 3.5×10^{-12} (90% C.L.) for solar axions. Assuming the Dine-Fischler-Srednicki-Zhitnitsky theoretical description, the upper limit in coupling corresponds to an upper limit on axion mass of 0.12 eV$/c^2$, while for the Kim-Shifman-Vainshtein-Zhakharov description masses above 36.6 eV$/c^2$ are excluded. For galactic axionlike particles, values of g_{Ae} larger than 4.2×10^{-13} are excluded for particle masses in the range 1–16 keV$/c^2$. These are the most stringent constraints to date for these interactions.

DOI: 10.1103/PhysRevLett.118.261301

Introduction.—The standard model of particle physics has long been thought to be incomplete as it is, for example, unable to explain dark matter, the observed matter-antimatter asymmetry of the universe, or the hierarchy problem. Another major weakness is the lack of a natural mechanism to explain the absence of charge-parity (CP) violation in strong interactions. A solution, introduced by Peccei and Quinn [1], postulates an additional global symmetry $U(1)_{\mathrm{PQ}}$ that is spontaneously broken at some large energy scale f_a. This generates a Nambu-Goldstone boson, the Weinberg-Wilczek *axion* [2,3], with a field that transforms as $a(x) \to a(x) + \alpha f_a$, where α is the phase of the introduced scalar field. If there is more than one global symmetry and, therefore, more than one Nambu-Goldstone boson, the particle corresponding to the excitation of the field combination is then the axion. Axions arising from symmetry breaking at electroweak scales have been discounted, having been ruled out by experimental searches [4], but axions that result from a much higher energy scale, so-called "invisible" axions [5–7], remain viable. In addition to QCD axions, particle excitations of the fields orthogonal to this field combination are called axionlike particles (ALPs), and indeed, numerous string-theory driven models predict ALP candidates [8–11].

Both axions and ALPs make interesting dark matter candidates [12]: they are nearly collisionless, neutral, nonbaryonic, and may be present in sufficient quantities to provide the expected dark matter density. Axions may have been produced as a nonthermal relic by the misalignment mechanism [13,14] and while very light, are predicted to be produced essentially at rest, thus satisfying the criteria for cold dark matter. There are also possible thermal production mechanisms [15], although these are unlikely to result in significant contributions to the dark matter. ALPs may have been present during the early phases of the Universe, produced as stable or long-lived particles that are now slowly moving within our Galaxy [16].

Production of axions may arise in stellar environments leading to a constant rate of emission from stars. From the Sun, this provides a second possible source of axion signal, but the consistency of stellar behavior with models that exclude axion emission also leads to tight constraints on their existence [17–19]. Additional constraints arise from searches for axion couplings to photons via the Primakoff effect [20,21]. Axions and ALPs are also expected to couple with electrons, so can be probed with a wider range of experimental techniques, such as instruments with germanium and xenon active targets [22,23]. Here we present searches for axioelectric coupling with the LUX experiment for two specific scenarios: (i) QCD axions emitted from the sun, and (ii) keV-scale galactic ALPs that could constitute the gravitationally bound dark matter.

Signal expectation in LUX.—The Large Underground Xenon experiment (LUX) provides sensitivity to dark matter in the form of weakly interacting massive particles (WIMPs), reporting, for example, the most sensitive limits to date for spin-independent and spin-dependent WIMP-neutron interactions for masses above 4 GeV/c^2 [24–27]. LUX is a dual-phase xenon time-projection chamber (TPC) consisting of a low-radioactivity titanium vessel partially filled with liquid xenon such that above the liquid a layer of gaseous xenon is maintained. A vertical electric field of 181 V/cm is established via a gate grid placed within the gas layer, and a cathode at the base of the liquid. The detector has an active target mass of 250 kg. Energy deposited by incident radiation creates a primary scintillation signal, called $S1$, and ionization charge. The latter, when drifted vertically in an electric field to produce an electroluminescence signal in the gas phase, leads to a delayed signal, called $S2$. Both signals are detected by photomultiplier tubes (PMTs), 61 viewing the TPC from above and 61 from below. The location at which an energy deposition occurred may be reconstructed from the distribution of signal sizes in the PMTs, which gives the position in the horizontal plane. The standard deviations of the reconstructed coordinates have a statistical contribution of 10 mm at the S2 threshold due to Poisson fluctuations in the numbers of detected photons. To this, a 5 mm systematic contribution is added, as estimated from events that arise from the well-defined wall position [25]. The period of delay (0–324 μs) between the $S1$ and the $S2$ then gives the vertical position, with a resolution of 0.9 mm [25]. The ionization threshold is sufficiently low to allow observation of single electrons emitted from the liquid surface, giving a very low energy threshold for experimental searches. A detailed description of the detector and its deployment at the Sanford Underground Research Facility may be found in Ref. [28].

Importantly, axion or ALP interactions in LUX would result in additional events within the electron-recoil class of events, identified principally by the ratio of $S2$ to $S1$ signal size. This is in contrast to searches for WIMPs that are conducted within the nuclear recoil band. Moreover, whereas the nuclear recoil band is essentially background free (dominated in fact by leakage from the electron recoil band), the electron recoil band is populated significantly, with contributions from gamma rays and beta particles from radioactive contaminations within the xenon, from the detector instrumentation, and from external environmental sources. Data presented here, and their analysis, come from the period April 24 to September 1, 2013, with a total exposure consisting of 118 kg fiducial mass over a 95 live-days period.

Axion and ALP searches rely on the so-called *axioelectric* effect [29–31],

$$\sigma_{\mathrm{Ae}} = \sigma_{\mathrm{pe}}(E_A)\frac{g_{\mathrm{Ae}}^2}{\beta_A}\frac{3E_A^2}{16\pi\alpha_{\mathrm{em}}m_e^2}\left(1-\frac{\beta_A^{2/3}}{3}\right), \qquad (1)$$

where σ_{pe} is the photoelectric cross section on the target material (xenon), g_{Ae} is the coupling constant between

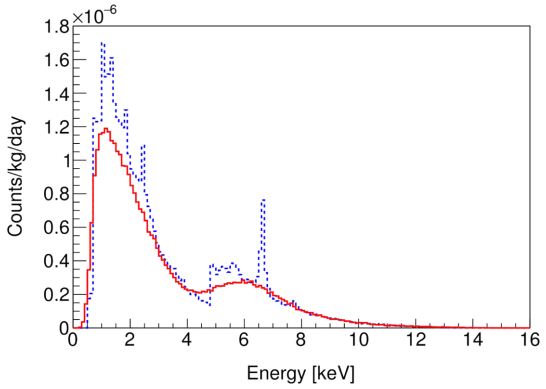

FIG. 1. Dashed blue distribution: expected energy spectrum from a massless solar axion, assuming a coupling $g_{Ae} = 10^{-12}$. The shape arises from the combination of a continuous contribution to the axion flux due to bremsstrahlung and Compton scattering, together with features associated with atomic recombination and deexcitation effects. Solid red distribution: The expected LUX experimental solar axion energy spectrum, as modeled with NEST [34–36].

axion or ALP and electron, α_{em} is the fine-structure constant, m_e is the mass of the electron, and β_A and E_A are the velocity and the energy of the axion.

Two signal sources are considered here: axions produced and emitted from the Sun, and primordial ALPs within the Galaxy. In the first case, Redondo [32] has estimated the solar axion spectral shape, assuming massless axions. The flux is dominated by contributions from atomic recombination and deexcitation (that introduce features associated with atomic shell structure), bremsstrahlung and Compton scattering (both of which contribute smoothly), and is presented as the dashed blue line in Fig. 1, for an arbitrary choice of axion coupling constant. The flux, as estimated for zero axion mass, is still valid without heavy corrections for masses smaller than 1 keV/c^2, since the total energy is dominated by kinetic energy. The solar axion is therefore approximated to be massless, but note that these models cover theoretically interesting phase space, including the region for which axions provide a solution to the strong CP problem. Such a signal detected in LUX would be modified by detector resolution and efficiency effects [33]. These have been modeled with the Noble Element Simulation Technique (NEST) package [34–36] with the resulting expected solar axion energy spectrum presented as the solid red distribution in Fig. 1.

In the case of ALP interactions within a detector, because the ALPs are expected to be essentially at rest within the galaxy, axioelectric absorption leads to electron recoils with kinetic energy equal to the mass of the ALP. Interactions of this type therefore produce a monoenergetic spectral feature.

Background model.—The detector design, its location deep underground, and its construction from radiopure materials contribute to ensuring a low rate of events from background radioactivity. Moreover, xenon attenuates radiation relatively strongly ($Z = 54$, density ~ 3 g/cm^2) which, combined with the ability to accurately reconstruct the position of the interaction point, allows fiducialization away from local sources of background such as the walls that surround the xenon target, the PMTs, and the cathode.

Figure 2 presents, for the fiducial volume and the energy region of interest, the LUX 2013 data, together with the background model. Radiogenic backgrounds are estimated as in Ref. [37] and lead to a contribution from Compton scattering of γ rays from detector component radioactivity (light green). An additional γ-ray contribution arising from heavily down-scattered emission from ^{238}U chain, ^{232}Th chain, and ^{60}Co decays in the center of a large copper block below the PMTs is also included [25] (dark green). Further significant contributions arise from ^{85}Kr and Rn-daughter contaminants in the liquid xenon undergoing β decay with no accompanying γ rays detected (orange), and x rays emitted following those ^{127}Xe electron-capture decays where the coincident γ ray escapes the xenon (purple). Each background contribution has been estimated from modeling measured impurity levels, and no scaling has been performed. The four observables used in the subsequent statistical analysis are modeled: the prompt scintillation ($S1$), the base 10 logarithm of the proportional ($S2$) signal, the radius (r), and depth (z) of the event location. $S1$ pulses are required to have two PMTs in coincidence and an $S1$ value in the range 1–80 detected photons; the $S2$ signal is required to be in the range 100–10 000 detected photons. A radial fiducial cut is placed at 18 cm and the range in z is set to be 48.6–8.5 cm above the faces of the bottom PMTs. The resulting fiducial volume has been calculated as in Ref. [24].

Figure 3 shows the background model and LUX 2013 data as a function of recoil energy, with energy reconstructed as $E = [S1_c/g_1 + S2_c/(\epsilon g_2)]W$. Here, $S1_c$ is the $S1$ signal size corrected to equalize the response throughout the active volume to the response at the center of the detector (scale of corrections $\pm 10\%$), while $S2_c$ is the $S2$ signals size corrected to equalize the response to that at the surface (scale of correction from 0 to 50%). $g_1 = 0.117 \pm 0.003$ phd/photon and $g_2 = 12.1 \pm 0.8$ phd/electron are the gain factors [38], defined by the expectation values $\langle S1 \rangle = g_1 n_\gamma$ and $\langle S2 \rangle = g_2 n_e$, where n_γ and n_e represent the initial number of photons and electrons produced by the interaction; $\epsilon = 49\% \pm 3\%$ [38] is the efficiency for extracting electrons from the liquid to the gas; and $W = (13.7 \pm 0.2)$ eV [38] is the work function for the production of either a photon or an electron.

Analysis.—Profile Likelihood Ratio analysis: A two-sided profile likelihood ratio (PLR) analysis [39] has been performed to test the signal models against the LUX 2013 data. The approach used is consistent with that applied to the LUX standard WIMPs search [25], in which the PLR is based on the simultaneous separation of the signal and the

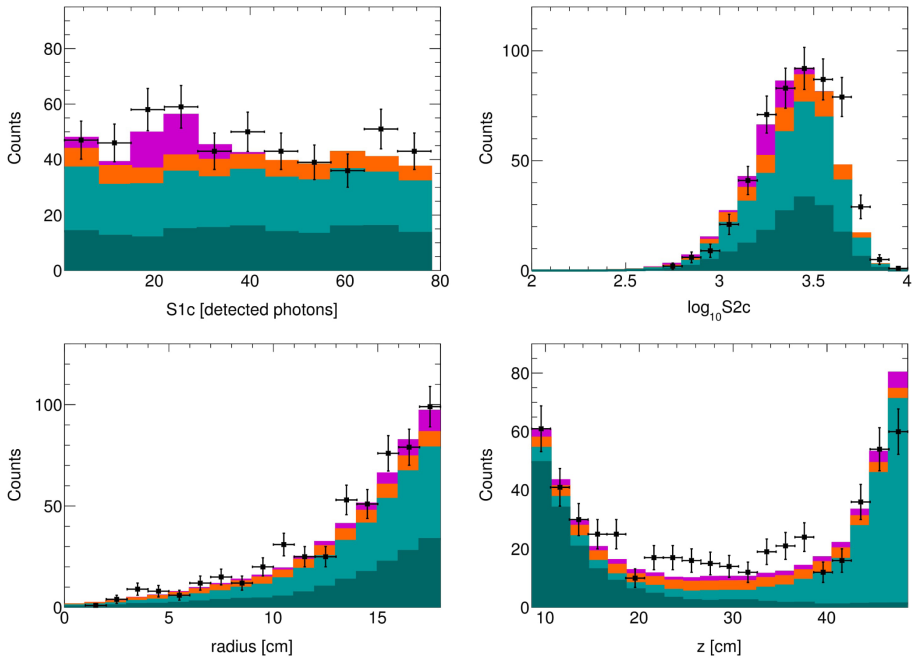

FIG. 2. LUX 2013 electron recoil data (filled black squares, with error bars) together with the background model, comprised of contributions from low-z-origin γ rays (dark green), other γ rays (light green), ^{85}Kr or Rn-daughter contaminants in the liquid xenon undergoing β decay (orange) and x rays due to ^{127}Xe (purple). The four panels show the distributions in terms of the four parameters used in the analysis: $S1_c$ (top left), $\log_{10}S2_c$ (top right), radial coordinate (bottom left), and vertical coordinate (bottom right). The number of counts in each background component is based on independent assay results and measurements, with no additional scaling.

background distributions in the four physical observables: r, z, $S1_c$, and $\log_{10}(S2_c)$. Conversion of theoretical axion and ALP energy spectra to probability density functions for each of the physical observables has been performed with NEST [34–36], taking into account the detector response and the efficiency. The models of the signal for the solar axions, and for an example 10 keV/c^2 mass galactic ALP, are shown in Fig. 4, projected on the two-dimensional space of $\log_{10} S2_c$ as a function of $S1_c$.

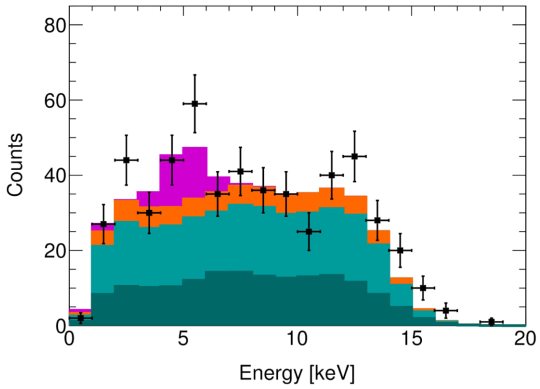

FIG. 3. Energy spectrum of the LUX 2013 electron recoil background. Data are filled black squares with error bars; the individual contributions to the background model are the stacked colored histograms: low-z-origin γ rays (dark green), other γ rays (light green), ^{85}Kr or Rn-daughter contaminants in the liquid xenon undergoing β decay (orange), x rays due to ^{127}Xe (purple). The number of counts in each background component is based on independent assay results and measurements, with no additional scaling. The cutoff at higher energies is due to the requirement on $S1$ signal size.

Systematic uncertainties in background rates are treated as nuisance parameters in the PLR. Table I summarizes the contributions from the background sources, listing the number of events expected in the total exposure and the best fit value returned by the PLR (in the solar axion search). The constraints are Gaussian distributions, with means and standard deviations indicated.

The PLR analysis extracts a 90% C.L. upper limit on the number of signal events: if the local p value is below 10%, the signal hypothesis is excluded at 90% C.L. The limit on the number of signal events is then converted to a limit on the coupling constant between axion/ALP and electrons, g_{Ae}.

The look elsewhere effect: The ALP study is conducted by searching for a specific feature over a range of masses. The local significance of observing such a feature at one particular mass must be moderated by the number of trials undertaken, in order to calculate a global significance [40]. In Fig. 5, the local p value, i.e., the probability of such an excess if there is no ALP signal at that mass, is plotted as a function of the ALP mass, highlighting the correspondence with the number of standard deviations (σ) away from the null hypothesis. At 12.5 keV/c^2 a local p value of 7.2×10^{-3} corresponds to a 2.4σ deviation. Following the procedure outlined in Ref. [41] (where it was applied to

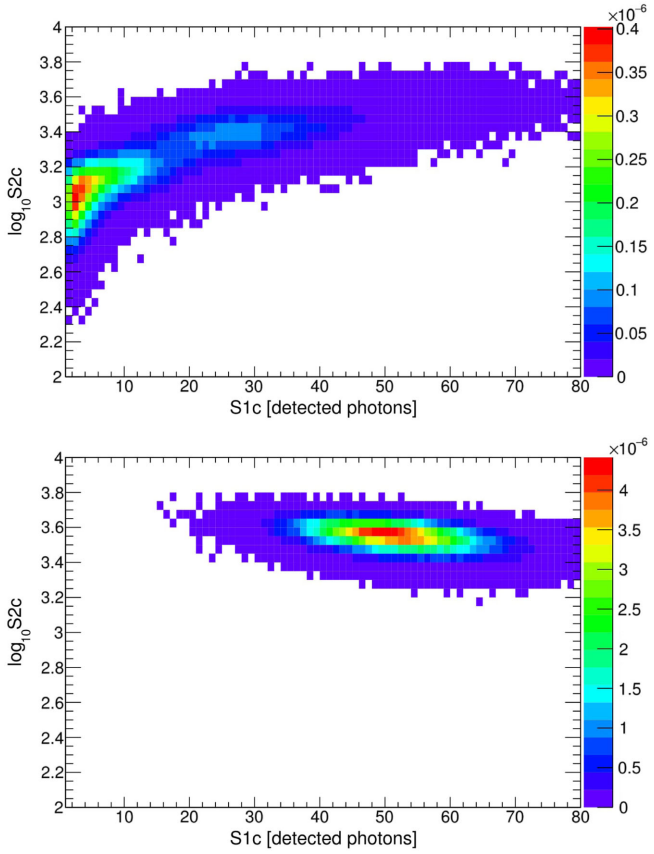

FIG. 4. Signal models projected on the two dimensional space of $\log_{10} S2_c$ as a function of $S1_c$, for massless solar axions (top) and 10 keV/c^2 mass galactic ALPs (bottom).

searches for the Higgs boson), a boost factor has been calculated that evaluates the likelihood of finding a deviation for a number of searches as compared to the significance that would apply to a search performed only once. Consequently, the global p value is evaluated as 5.2×10^{-2} at 12.5 keV/c^2, corresponding to a 1.6σ rejection of the null hypothesis.

Results.—The 90% C.L. upper limit on the coupling g_{Ae} between solar axions and electrons is shown in Fig. 6, along with the limits set by the previous experiments [19,23,42,43], the astrophysical limit set via the Red Giant cooling process [18] and the theoretical models

TABLE I. Nuisance parameters in the best fit to the 2013 LUX data for solar axions. Constraints are Gaussian with means and standard deviations indicated. Events counts are after analysis cuts and thresholds, as described in Ref. [25].

Parameter	Constraint	Fit value (solar axions)
Low-z-origin γ counts	161 ± 69	157 ± 17
Other γ counts	223 ± 96	175 ± 18
β counts	67 ± 27	113 ± 18
^{127}Xe counts	39 ± 12	42 ± 8

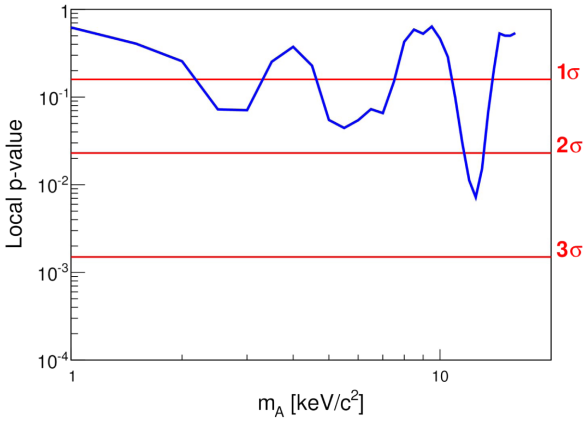

FIG. 5. Local p value as a function of the ALP mass. The minimum is reached at 12.5 keV/c^2, where the local p value is 7.2×10^{-3}, corresponding to a 2.4σ local deviation.

describing QCD axions [5–7]. The 2013 LUX data set excludes a coupling larger than 3.5×10^{-12} at 90% C.L, the most stringent such limit so far reported. Assuming the Dine-Fischler-Srednicki-Zhitnitsky model, which postulates the axion as the phase of a new electroweak singlet scalar field coupling to a new heavy quark, the upper limit in coupling corresponds to an upper limit on axion mass of 0.12 eV/c^2, while for the Kim-Shifman-Vainshtein-Zhakharov description, which assumes the axion interacting with two Higgs doublets rather than quarks or leptons, masses above 36.6 eV/c^2 are excluded.

In the galactic ALP study, a scan over masses has been performed, within the range of 1–16keV/c^2, limited by the range over which precise knowledge of light and charge yield is determined through tritiated methane calibration data [33]. Assuming that ALPs constitute all of the galactic dark matter, the 90% C.L. upper limit on the coupling between ALPs and electrons is shown in Fig. 7 as a function of the mass, together with the results set by other

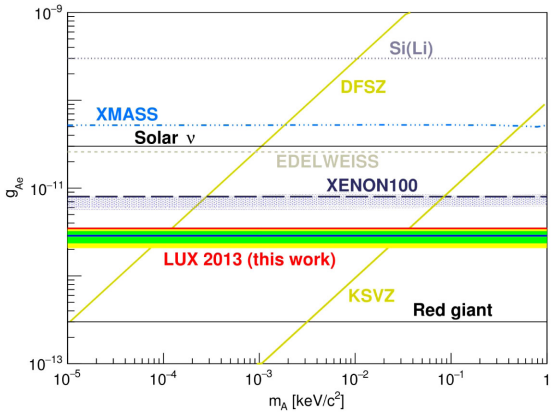

FIG. 6. Red curve: LUX 2013 data 90% C.L. limit on the coupling between solar axions and electrons. Blue curve: 90% C.L. sensitivity, $\pm 1\sigma$ (green band), and $\pm 2\sigma$ (yellow band).

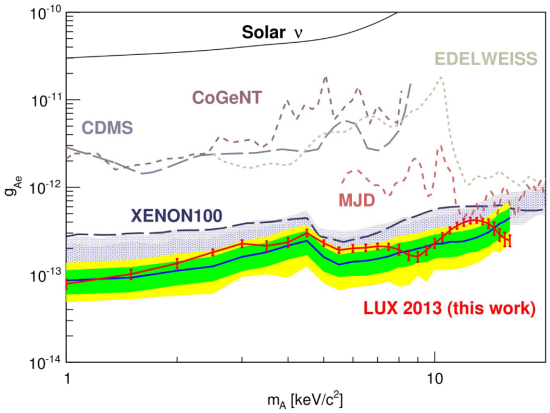

FIG. 7. Red curve: LUX 2013 data 90% C.L. limit on the coupling between galactic axionlike particles and electrons. Blue curve: 90% C.L. sensitivity, $\pm 1\sigma$ (green band), and $\pm 2\sigma$ (yellow band).

experiments [19,23,42,44–46]. Again, this is the most stringent such limit so far reported in this mass range.

Summary.—We have presented the results of the first axion and ALP searches with the LUX experiment. Under the assumption of an axioelectric effect interaction in xenon, we test the coupling constant between axions and ALPs with electrons, g_{Ae}, using data collected in 2013, for a total exposure of 95 live days $\times 118$ kg. Using a profile likelihood ratio statistical analysis, for solar axions we exclude g_{Ae} larger than 3.5×10^{-12} (90% C.L.) and axion masses larger than 0.12 or 36.6 eV$/c^2$ under the assumption of the Dine-Fischler-Srednicki-Zhitnitsky or Kim-Shifman-Vainshtein-Zhakharov theoretical models, respectively. For axionlike particles, a scan over masses within the range 1–16 keV$/c^2$ excludes discovery of a signal with a global significance at a level of 1.6σ, and constrains values of the coupling to be no larger than 4.2×10^{-13}, across the full range.

This work was partially supported by the U.S. Department of Energy under Awards No. DE-AC02-05CH11231, No. DE-AC05-06OR23100, No. DE-AC52-07NA27344, No. DE-FG01-91ER40618, No. DE-FG02-08ER41549, No. DE-FG02-11ER41738, No. DE-FG02-91ER40674, No. DE-FG02-91ER40688, No. DE-FG02-95ER40917, No. DE-NA0000979, No. DE-SC0006605, No. DE- SC0010010, and No. DE-SC0015535, the U.S. National Science Foundation under Grants No. PHY-0750671, No. PHY-0801536, No. PHY-1003660, No. PHY-1004661, No. PHY-1102470, No. PHY-1312561, No. PHY-1347449, No. PHY-1505868, and No. PHY-1636738, the Research Corporation Grant No. RA0350, the Center for Ultra-low Background Experiments in the Dakotas, and the South Dakota School of Mines and Technology. LIP-Coimbra acknowledges funding from Fundação para a Ciência e a Tecnologia through the Project-Grant No. PTDC/FIS-NUC/1525/2014. Imperial College and Brown University thank the UK Royal Society for travel funds under the International Exchange Scheme (Grant No. IE120804). The UK groups acknowledge institutional support from Imperial College London, University College London, and Edinburgh University, and from the Science & Technology Facilities Council for Ph.D. studentships Grants No. ST/K502042/1 (A. B.), ST/ K502406/1 (S. S.), and ST/M503538/1 (K. Y.). The University of Edinburgh is a charitable body registered in Scotland, with Registration No. SC005336. We gratefully acknowledge the logistical and technical support and the access to laboratory infrastructure provided to us by SURF and its personnel at Lead, South Dakota. SURF was developed by the South Dakota Science and Technology Authority, with an important philanthropic donation from T. Denny Sanford, and is operated by Lawrence Berkeley National Laboratory for the Department of Energy, Office of High Energy Physics.

*Corresponding author.
m.marzioni@ed.ac.uk

[1] R. D. Peccei and H. R. Quinn, Phys. Rev. Lett. **38**, 1440 (1977).
[2] S. Weinberg, Phys. Rev. Lett. **40**, 223 (1978).
[3] F. Wilczek, Phys. Rev. Lett. **40**, 279 (1978).
[4] J. E. Kim and G. Carosi, Rev. Mod. Phys. **82**, 557 (2010).
[5] M. Dine, W. Fischler, and M. Srednicki, Phys. Lett. **104B**, 199 (1981).
[6] J. E. Kim, Phys. Rev. Lett. **43**, 103 (1979).
[7] M. A. Shifman, A. I. Vainshtein, and V. I. Zakharov, Nucl. Phys. **B166**, 493 (1980).
[8] E. Witten, Commun. Math. Phys. **92**, 455 (1984).
[9] J. P. Conlon, J. High Energy Phys. 05 (2006) 078.
[10] A. Arvanitaki, S. Dimopoulos, S. Dubovsky, N. Kaloper, and J. March-Russell, Phys. Rev. D **81**, 123530 (2010).
[11] M. Cicoli, M. D. Goodsell, and A. Ringwald, J. High Energy Phys. 10 (2012) 146.
[12] L. Abbott and P. Sikivie, Phys. Lett. **120B**, 133 (1983).
[13] J. Preskill, M. Wise, and F. Wilczek, Phys. Lett. **120B**, 127 (1983).
[14] M. Dine and W. Fischler, Phys. Lett. **120B**, 137 (1983).
[15] A. Salvio, A. Strumia, and W. Xue, J. Cosmol. Astropart. Phys. 01 (2014) 011.
[16] F. D. Steffen, Eur. Phys. J. C **59**, 557 (2009).
[17] J. Isern *et al.*, arXiv:1304.7652v1.
[18] N. Viaux, M. Catelan, P. B. Stetson, G. G. Raffelt, J. Redondo, A. A. R. Valcarce, and A. Weiss, Phys. Rev. Lett. **111**, 231301 (2013).
[19] P. Gondolo and G. G. Raffelt, Phys. Rev. D **79**, 107301 (2009).
[20] S. J. Asztalos *et al.* (ADMX Collaboration), Phys. Rev. Lett. **104**, 041301 (2010).
[21] M. Arik *et al.* (CAST Collaboration), Phys. Rev. Lett. **112**, 091302 (2014).
[22] K. Arisaka, P. Beltrame, C. Ghag, J. Kaidi, K. Lung, A. Lyashenko, R. D. Peccei, P. Smith, and K. Ye, Astropart. Phys. **44**, 59 (2013).

[23] E. Aprile *et al.* (XENON100 Collaboration). Phys. Rev. D **95**, 029904 (2017).
[24] D. S. Akerib *et al.* (LUX Collaboration), Phys. Rev. Lett. **112**, 091303 (2014).
[25] D. S. Akerib *et al.* (LUX Collaboration), Phys. Rev. Lett. **116**, 161301 (2016).
[26] D. S. Akerib *et al.* (LUX Collaboration), arXiv:1705.03380.
[27] D. S. Akerib *et al.* (LUX Collaboration), Phys. Rev. Lett. **118**, 021303 (2017).
[28] D. S. Akerib *et al.* (LUX Collaboration), Nucl. Instrum. Methods Phys. Res., Sect. A **704**, 111 (2013).
[29] G. D. Starkman, S. Dimopoulos, and B. W. Lynn, Phys. Lett. **168B**, 145 (1986).
[30] A. Derevianko, V. A. Dzuba, V. V. Flambaum, and M. Pospelov, Phys. Rev. D **82**, 065006 (2010).
[31] M. Pospelov, A. Ritz, and M. Voloshin, Phys. Rev. D **78**, 115012 (2008).
[32] J. Redondo, J. Cosmol. Astropart. Phys. 12 (2013) 008.
[33] D. S. Akerib *et al.* (LUX Collaboration), Phys. Rev. D **93**, 072009 (2016).
[34] M. Szydagis, N. Barry, K. Kazkaz, J. Mock D. Stolp M. Sweany M. Tripathi, S. Uvarov, N. Walsh, and M. Woods, J. Instrum. **6**, P10002 (2011).
[35] M. Szydagis, A. Fyhrie, D. Thorngren, and M. Tripathi J. Instrum. **8**, C10003 (2013).
[36] B. Lenardo, K. Kazkaz, A. Manalaysay, J. Mock, M. Szydagis, and M. Tripathi IEEE Trans. Nucl. Sci. **62**, 3387 (2015).
[37] D. S. Akerib *et al.* (LUX Collaboration), Astropart. Phys. **62**, 33 (2015).
[38] D. S. Akerib *et al.* (LUX Collaboration), Phys. Rev. D **95**, 012008 (2017).
[39] G. Cowan, K. Cranmer, E. Gross, and O. Vitells, Eur. Phys. J. C **71**, 1554 (2011).
[40] E. Gross and O. Vitells, Eur. Phys. J. C **70**, 525 (2010).
[41] CMS Collaboration, Phys. Lett. B **716**, 30 (2012).
[42] E. Armengaud *et al.* J. Cosmol. Astropart. Phys. 11 (2013) 067.
[43] K. Abe *et al.* Phys. Lett. B **724**, 46 (2013).
[44] N. Abgrall *et al.* (MAJORANA Collaboration), Phys. Rev. Lett. **118**, 161801 (2017).
[45] CDMS Collaboration, Phys. Rev. Lett. **103**, 141802 (2009).
[46] C. E. Aalseth *et al.* (CoGeNT Collaboration), Phys. Rev. Lett. **101**, 251301 (2008).